WILEY ONLINE LIBRARY EarlyView publication on wileyonlinelibrary.com (issue and page numbers not yet assigned; citable using Digital Object Identifier – DOI)

Phys. Status Solidi A, 1–6 (2013) / DOI 10.1002/pssa.201300059

Part of Topical Section on Fundamentals and Applications of Diamond and Nanocarbons

physica status solidi a
www.pss-a.com
applications and materials science

Influence of diamond-like carbon overlay properties on refractive index sensitivity of nano-coated optical fibres

Mateusz Śmietana[*,1], Mariusz Dudek[,2], Marcin Koba[***,1,3], and Bartosz Michalak[****,1]**

[1] Institute of Microelectronics and Optoelectronics, Warsaw University of Technology, Koszykowa 75 00-662, Warsaw, Poland
[2] Institute of Materials Science and Engineering, Lodz University of Technology, Stefanowskiego 1/15 90-924, Lodz, Poland
[3] National Institute of Telecommunications, Szachowa 1, 04-894 Warsaw, Poland

Received 11 April 2013, revised 10 May 2013, accepted 10 May 2013
Published online 12 August 2013

Keywords diamond-like carbon, optical fibre sensors, optical properties, refractive index sensing, RF PECVD, thin film

[*] Corresponding author: m.smietana@elka.pw.edu.pl, Phone: +48 22 234 6364, Fax: +48 22 234 6063
[**] e-mail mariusz.dudek@p.lodz.pl, Phone: +48 42 631 3263 ext. 31, Fax: +48 42 636 6790
[***] e-mail m.koba@elka.pw.edu.pl, Phone: +48 22 234 7246, Fax: +48 22 234 6063
[****] e-mail b.michalak@stud.elka.pw.edu.pl, Phone: +48 22 234 6364, Fax: +48 22 234 6063

An application of diamond-like carbon (DLC) nano-coated optical fibre as a promising platform for external medium refractive index (RI) sensing is investigated. The DLC thin films are deposited by radio frequency plasma enhanced chemical vapour deposition (RF PECVD) on fused-silica core ($\varnothing = 400$ μm) of multimode polymer-clad silica (PCS) optical fibres. The optical fibre sensor response to variations of the external RI for samples coated with DLC film for various thickness and optical properties of the film is measured, and compared to numerical simulations. We show that both optical properties and thickness of the DLC films depend on the deposition time. The effect has a strong impact on the optical response of the samples to variations of the external RI. The response is mainly influenced by the thickness and RI of the DLC overlay. Moreover, the response also depends on the investigated wavelength range. We show that for intensity-based configuration at $\lambda \sim 490$ nm, the DLC film thickness should reach about 80 nm. In such a configuration the sensitivity reaches over 2000% per RI unit (RIU). For wavelength-based configuration, when shift of the intensity deep at $\lambda \sim 490$ nm is considered, the thickness of the film should be as high as 120 nm. In such a configuration the sensitivity reaches 250 nm RIU^{-1}.

1 Introduction There is a great interest in application of optical fibre sensors, especially in places where traditional electronic or mechanical sensors cannot work due to harsh environmental conditions [1]. One of the simplest optical fibre sensing structure is based on short length (tens of mm) of core of the fibre exposed to external media [2]. In such a configuration evanescent wave interacts with the external media resulting in modulation of the light intensity guided in the fibre. In more advanced structures, the core is coated by an overlay which typically absorbs or binds certain stimulant. The phenomenon induces variations of optical properties of the overlay, and thus modification in light propagation conditions in the optical structure [3]. There is another group of sensors which are coated with an overlay showing higher refractive index (RI, n) than the one of the fibre core. For these sensors, the overlay at its certain thickness can modify the response of the optical fibre structure to external RI. Such a sensing device offers simplicity of fabrication and flexibility in determining its functionality by proper selection of the applied properties of the overlay. Moreover, the device offers high sensitivity, which rivals some more complex optical structures [4]. A number of materials, including TiO_2, In_2O_3, ITO and some polymers, has been applied for discussed optical fibre sensing configuration [4–6]. The overlays have been deposited from liquid precursors by dip coating method. An application of vapour deposition methods for this purpose which offer wide selection of materials and possibility of *in situ* tuning of their properties is rare. In our previous works we have shown a capability for

deposition of diamond-like carbon (DLC) overlay on optical fibres [7]. DLC is a form of amorphous carbon or hydrogenated amorphous carbon exhibiting high hardness and good resistance to chemical corrosion [8]. DLC is typically applied for passivation or protection of various tools and devices [9]. DLC applied for electronic devices can play a role of diffusion barrier against water molecules and sodium ions, two major sources of corrosion and instability in microelectronics [10]. In optical devices, DLC is typically applied as both protecting and antireflecting coating [11]. Some advanced optical sensors has also been demonstrated, where doped DLC has been used as a platform for RI sensing [12]. One of the biggest advantages of DLC is comparing to *e.g.* diamond, its deposition at low temperatures, which reduces the possibility of damaging substrate material. In our works we applied radio frequency plasma enhanced chemical vapour deposition (RF PECVD) method for deposition of these hard, smooth and wear resistant nano-overlays. It is also worth mentioning that DLC films show good adhesion to fused silica glass, which additionally makes them a good candidate for overlays enhancing sensing properties of the optical fibre devices. Our up to date investigations were based on measurements of power transmission at a narrow wavelength range ($\lambda \sim 620$ nm). We have already shown the capability of tuning the RI sensitivity by proper selection of the DLC overlay properties [13]. Recently it has been shown by other authors that the sensitivity in such a sensing configuration highly depends on the properties of the overlay, and what is more on wavelength range where the response is measured [14].

In this paper we discuss the influence of DLC film properties on the RI sensitivity in wide spectral range (λ from 350 to 1050 nm) in order to find optimal interrogation conditions for the sensor. Our experimental data are supported by simulations based on developed numerical model. The simulations allow for further improvement of the device sensitivity, especially by proper selection of DLC overlay properties.

2 Experimental details

2.1 Modelling and simulations The numerical model has been developed according to the fibre structure cross-section schematically shown in Fig. 1. The fibre has been excited by a polychromatic light source at input power P_{in}. The output spectrum $P_{out}(\lambda)$ is dependent on DLC nano-coating properties and optical properties of the external medium at the sensing region.

To determine the effective transmitted power (P_{out}) we employed Eq. (1), which is commonly used for surface plasmon resonance sensors [15, 16]. This formula was improved in comparison to some other shown in, *e.g.* [5, 6, 14], by taking into account not only meridional rays at angle of incidence in range from critical angle θ_c to $\pi/2$, where θ_c is expressed by Eq. (2), but also skew rays in range from 0 to $\alpha_{max} = \pi/2$ [15, 16]. At the maximum angle value, all the meridional and skew rays contribute to the P_{out}. In Eq. (1), $N(\theta, \alpha)$ denotes the total number of reflection in the fibre core in the region coated by DLC overlay, and is expressed by Eq. (3), where L is the length of the DLC region, D the core diameter, α the skewness angle and θ is the angle shown in Fig. 1. The P_{in} represents the power at the fibre input, which for wide light source can be represented according to Eq. (4). It must be noted here that since in discussed case $\varepsilon_r > 0$, $\varepsilon_r > |\varepsilon_i|$ and $\varepsilon_r > \varepsilon_{out}$, where ε_r, ε_i and ε_{out} are, respectively, DLC's real, imaginary and surrounding dielectric permittivity, then the film supports a lossy guided mode, which exists both for transverse electric (TE) and magnetic (TM) polarizations [17]. Finally, R in Eq. (1) represents averaged reflectivity of TM and TE modes given in Eq. (5).

$$P_{out} = \frac{\int_o^{\alpha_{max}} \int_{\theta_c}^{\pi/2} R^{N(\theta,\alpha)} P_{in} \mathrm{d}\theta \mathrm{d}\alpha}{\int_o^{\alpha_{max}} \int_{\theta_c}^{\pi/2} P_{in} \mathrm{d}\theta \mathrm{d}\alpha}, \tag{1}$$

$$\theta_c = \sin^{-1}\left(\frac{n_{cladding}}{n_{core}}\right), \tag{2}$$

$$N(\theta,\alpha) = \frac{L}{D \cos\alpha \tan\theta}, \tag{3}$$

$$P_{in} \propto n_0^2 \sin\theta \cos\theta, \tag{4}$$

$$R^{N(\theta,\alpha)} = \frac{R_{TM}^{N(\theta,\alpha)}(\theta,\alpha) + R_{TE}^{N(\theta,\alpha)}(\theta,\alpha)}{2}. \tag{5}$$

In order to obtain reflectivity for TM and TE polarized light, we perform calculations based on the transfer matrix method (TMM) for the multilayer structure shown Fig. 2.

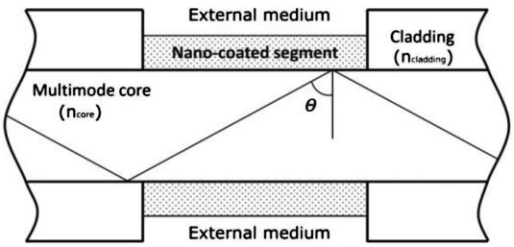

Figure 1 The cross-section of the investigated fibre sensor structure.

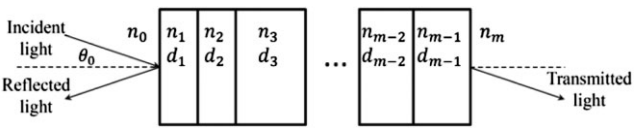

Figure 2 Schematic multilayer model used to determine the reflectivity.

In our model the ith layer is described by the RI n_i and thickness d_i. All the layers are assumed to be uniform and isotropic. The light inputs the first interface at an arbitrary angle θ_0. The tangential fields at the first boundary are related to those at the final boundary according to Eq. (6) where E_0 and H_0 are the tangential components of electric and magnetic fields at the first interface, respectively, M is the characteristic matrix of the structure, and E_{m-1} and H_{m-1} are the fields at the last interface.

$$\begin{bmatrix} E_0 \\ H_0 \end{bmatrix} = M \begin{bmatrix} E_{m-1} \\ H_{m-1} \end{bmatrix}, \tag{6}$$

$$M = \sum_{i-1}^{m-1} M_i = \begin{bmatrix} M_{11}\, M_{12} \\ M_{21}\, M_{22} \end{bmatrix}. \tag{7}$$

In Eq. (7) the M_i is described by Eq. (8), where β_i and q_i for TM and TE polarization and given by Eqs. (9), (10) and (11), respectively.

$$M_i = \begin{bmatrix} \cos\beta_i & (-i\sin\beta_i)/q_i \\ (-iq_i\ \sin\beta_i) & \cos\beta_i \end{bmatrix}. \tag{8}$$

$$\beta_i = \frac{2\pi d_i}{\lambda}\left(n_i^2 - n_0^2\sin^2\theta_0\right)^{1/2}, \tag{9}$$

$$q_i = \frac{\left(n_i^2 - n_0^2\sin^2\theta_0\right)^{1/2}}{n_i^2}, \tag{10}$$

$$q_i = \left(n_i^2 - n_0^2\sin^2\theta_0\right)^{1/2}. \tag{11}$$

Finally, the reflectivity at wavelength λ is given by Eq. (12). This equation is used to obtain expressions for the reflectivity of TM and TE polarizations.

$$R(\theta,\lambda) = |r|^2 = \left|\frac{(M_{11} + M_{12}q_m)q_0 - (M_{21} + M_{22}q_m)}{(M_{11} + M_{12}q_m)q_0 + (M_{21} + M_{22}q_m)}\right|^2. \tag{12}$$

In our investigations we use three layers: core of the fibre ($i = 0$), DLC nano-overlay ($i = 1$), and external medium ($i = 2$). The results of the reflectivity contributing to structure's transmission for various RI were normalized using data obtained for each sample in the air ($n_D = 1$).

2.2 Sensor fabrication In the experiment polymer-clad silica (PCS) multimode optical fibre ($\varnothing_{core} = 400$ μm) has been used. Outer polymer coating from 25 mm-long segment of the fibre (total length of the fibre is 150 mm) was mechanically and chemically stripped [7]. The stripped section of the silica core was cleaned in organic solvent before the overlay deposition.

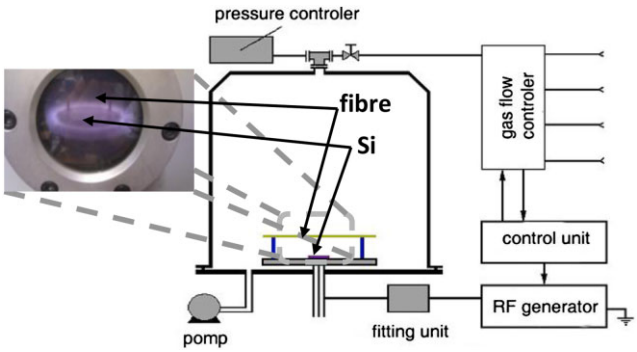

Figure 3 Scheme of the RF PECVD setup applied for DLC deposition on optical fibres and reference Si wafers.

The RF PECVD setup used for DLC deposition is schematically shown in Fig. 3. The fibres were suspended in a reactor chamber 5 mm over the RF electrode and reference oxidized silicon wafers were placed directly on the electrode. The deposition parameters were optimized for good adhesion of the films to silicon dioxide (SiO_2) substrates [18]. Each deposition was preceded by 5 min long ion sputtering in RF plasma discharge at negative self-bias voltage (V_B) of 300 V and residual pressure of 13 Pa. The deposition processes were performed at 30 sccm methane flow, pressure of 35 Pa and $V_B = 200$ V. The deposition time range was from 1 to 13 min.

2.3 Thin film and sensor characterization DLC film properties were investigated on reference Si samples using Horiba–Jobin–Yvon UVISEL spectroscopic ellipsometer (SE) in the wavelength range from 260 to 830 nm. The thickness and optical constants, *i.e.* n and extinction coefficient (k) were calculated by fitting of SE data using single layer Tauc–Lorenc model of DLC film [18].

The transmission of the optical fibre samples was measured in λ range from 350 to 1050 nm using Yokogawa AQ4305 white light source and Ocean Optics USB4000-VIS-NIR spectrometer. The applied measurement setup is schematically shown in Fig. 4. The nano-coated segment

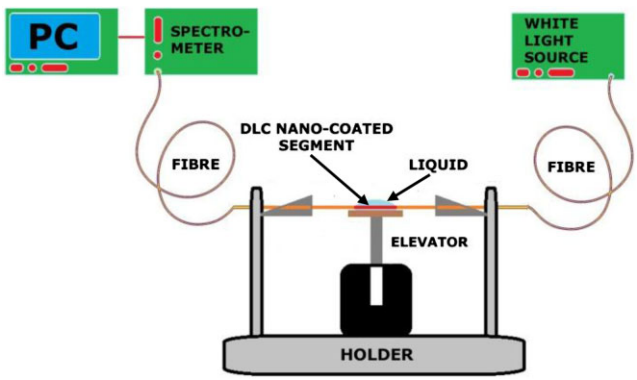

Figure 4 Scheme of the experimental setup applied for external RI measurements.

was immersed in various liquids prepared by mixing water and glycerine. The RI of the obtained liquid (n_D) was measured using Reichert AR200 Automatic Digital Refractometer. Wavelength-dependent response of the structures to variations in external RI was normalized using spectrum obtained for each sample surrounded by the air ($n_D = 1$).

3 Results and discussion The optical properties of the DLC film can be determined at the deposition stage by proper adjustment of a number of RF PECVD parameters, which include pressure in the chamber, gas flow and composition, self-bias voltage, temperature and deposition time [18]. Evolution of the DLC film thickness and optical properties with RF PECVD time is shown in Fig. 5. We obtained deposition rate reaching 11.8 nm min^{-1} and optical properties of the film, which are highly dependent on deposition time. The obtained deposition rate allows for good control of thickness of the deposited films. It is shown in Fig. 5b that the films reach the highest n when deposited in a 7 min long process. For process length up to 7 min, the n increases with deposition time, whereas for longer processes it starts to decrease. A similar trend is observed for k where for 7 min long process k is the highest and the lowest in λ range below and above ~420 nm, respectively. The influence of deposition time on optical properties of the films has been discussed in details elsewhere [19]. The effect is based on densification of the film in initial stage of its growth and then release of hydrogen promoted by increase of temperature during the process. A significant influence of deposition time on both DLC optical properties and thickness makes difficult independent determination of these parameters.

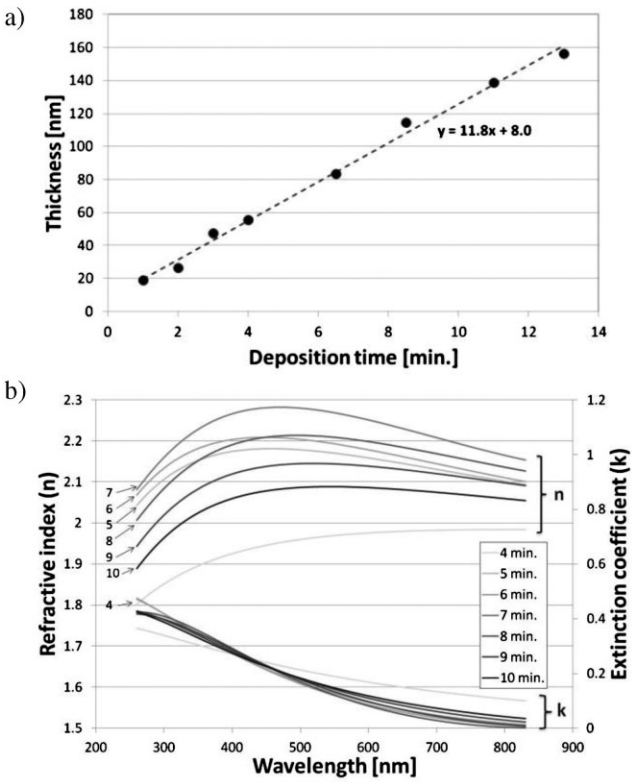

Figure 5 Evolution of DLC film (a) thickness and (b) optical properties, *i.e.* n and k, with deposition time.

It must be noted here that for the needs of the experiment, the properties of the DLC films were determined on reference Si wafers, not directly on the fibres. Due to the specificity of PECVD method applied in our work, we may expect the films to be slightly different in properties on fibres and on reference Si wafers. However, microscopic images of the fibre cross-section (not shown here) confirm good agreement between thickness of the film on the reference wafers and average thickness of the overlay on the fibres. Paying attention to this measurements and having in mind a possible imprecision in determination of the overlay properties on the fibre, in the following discussion we mention properties of the overlays and refer more to deposition time and estimated thickness of the overlay than precisely defined thickness of the overlay on the fibre.

Taking into consideration dispersion curves of n and k obtained for 4 min long deposition, we simulated the influence of the DLC film thickness on sensor's response to its immersion in water ($n_D = 1.3330$). It is shown in Fig. 6a that the maximum of transmitted power shifts towards longer wavelength with DLC thickness. The effect takes place in the investigated wavelength range up to 150 nm in film thickness. Another maximum appears at DLC thickness above 250 nm, but it is lower in intensity than the one for thinner films, and it shifts less in wavelength with increase of the thickness. Depending on thickness of the DLC, the transmitted power in selected wavelength ranges increases by over 100% as a result of immersing the sample in water. Next, in order to investigate the influence of n and k on sensor's response to immersing in water, we set film's thickness to 80 nm, and modified n and k dispersion curves by adding to them constant values. It is seen in Fig. 6b that the transmission maximum also shifts towards longer wavelength with increase of n. Simultaneously, it broadens its wavelength band and experiences reduction in intensity. The weakest effect to the sensors response has the increase of k shown in Fig. 6c. A significant increase in k (by 0.3) results in slight shift of the transmission maximum towards longer wavelength and broadening of its band. Taking into consideration that for investigated DLC films k variations are limited to 0.1, the effect resulting from its changes from one film to another can be neglected. Proper selection of overlay's n, and especially its thickness is critical from the point of view of the developed sensor performance.

Response of the DLC nano-coated samples to variations in external RI from 1 to 1.444 has been investigated next. The results obtained for three of the most representative samples are shown in Fig. 7. Depending mainly on DLC overlay thickness, the spectral response of the samples to changes in external RI is very different. In case of short depositions (<4 min, resulting in overlays below 50 nm in thickness) mainly a decrease in transmitted power is observed with increase in external RI. For longer depositions, the

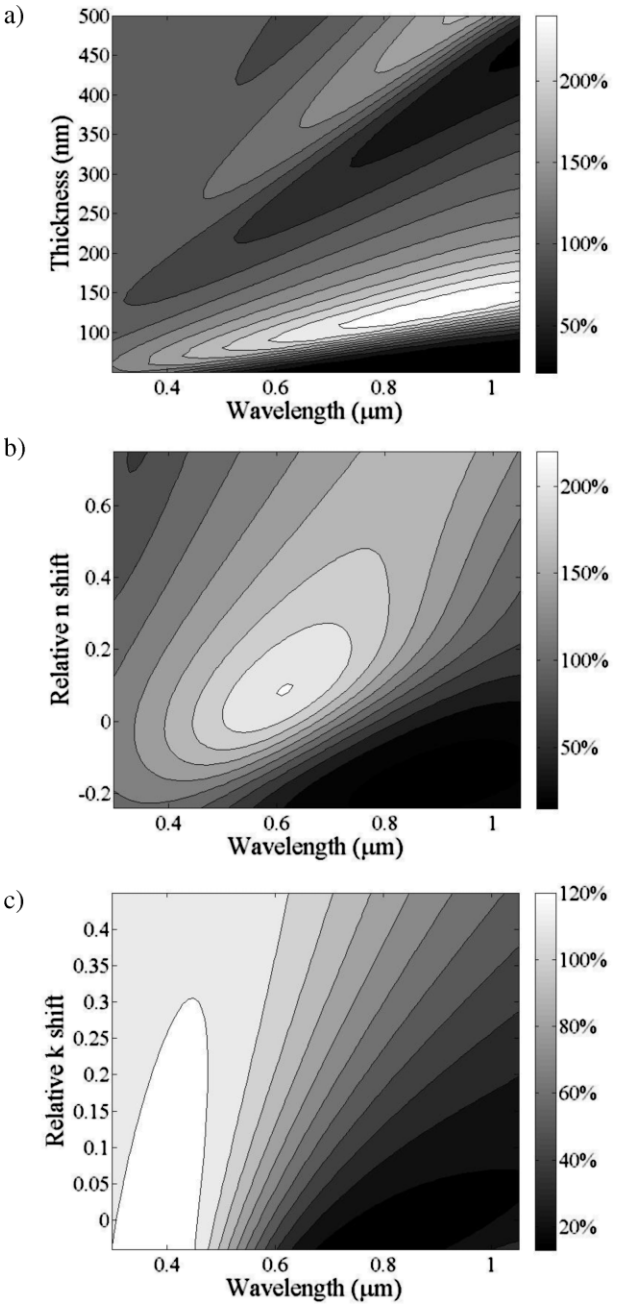

Figure 6 Influence of the DLC (a) thickness, (b) n and (c) k on transmission of the coated structure when external RI changes from 1 to 1.3330. Simulations were performed for (a) experimental data of n and k at 4 min long process. For (b) and (c) thickness was 80 nm.

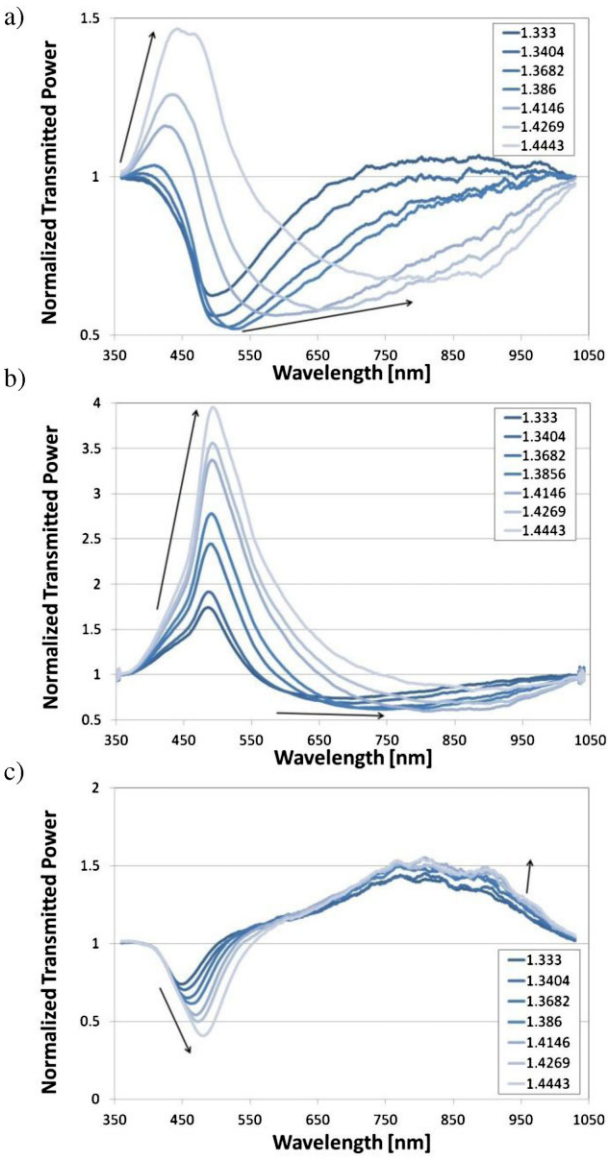

Figure 7 Influence of the external RI on transmission of the DLC-coated structures normalized to response recorded in air, where (a), (b) and (c) represent the effect for 4, 6.5 and 10 min long DLC deposition time.

transmitted power starts to increase in the lower wavelength range and shifts towards longer wavelength with RI.

When the thickness of the DLC overlay reaches about 80 nm a dynamic increase in transmitted power with RI at $\lambda \sim 490$ nm is observed. The sensitivity defined as variations in normalized transmitted power per RI unit (RIU) reaches here 2000% RIU^{-1} and is linear in the whole investigated RI range. For thicker DLC films (>100 nm) the maximum transmitted power further shifts towards longer wavelength, significantly losing its intensity and becoming insensitive to RI. But at shorter wavelength minimum of transmitted power appears, which shift towards longer wavelength with RI. Sensitivity defined as shift in wavelength of the power minimum per RIU reaches here 250 nm RIU^{-1}. For samples with thicker DLC overlay, the observed phenomenon is similar to the one noticed for samples with a very thin film. It proves the periodicity observed and discussed, in case of the results of simulations for the thickness variations.

4 Conclusions Besides typical application of DLC for mechanical and chemical protection of various surfaces, the material can be successfully applied for tuning sensitivity of optical fibre devices. Presented approach is based on multimode optical fibre with a 25-mm-long segment of removed cladding where the core is coated with the DLC nano-overlay. Relatively low-temperature process allows for DLC deposition on polymer-coated fibres. Thin, smooth and high-RI ($n > 1.8$) films were deposited on the sidewalls of the fibre using RF PECVD method. The properties of the DLC films can be easily modified by proper selection of the deposition process parameters. Applied numerical model, performed simulations and experimental data confirm the influence of thickness and optical properties of DLC on sensor's RI response. Depending on chosen interrogation method, which can be based on variations in transmitted power at fixed wavelength or shift of the transmitted power minimum in wavelength, a proper thickness of the DLC should be deposited. For the DLC film thickness of about 80 nm, and at fixed $\lambda = 490$ nm, variations in the transmitted power with external RI reaches 2000% RIU^{-1} where for thicker overlays ($\sim$120 nm in DLC thickness) the wavelength of the transmission minimum reaches the sensitivity of 250 nm RIU^{-1}.

In contrast to other films applied for such devices, which are typically deposited with dip coating methods, applied in this work RF PECVD method allows for repeatable and time efficient fabrication of the device. Its application is cheap when mass fabrication is considered. The platform seems to be very promising for application in label-free bio-sensing. This approach allows for application of a chemically or biologically sensitive film on top of the nano-coating, resulting in developing of both a highly sensitive and selective device.

Acknowledgements The authors gratefully acknowledge support for this work from the National Centre for Research and Development of Poland within the LIDER program.

References

[1] F. T. S. Yo, and S. Yin (eds.), Fiber Optic Sensors (Marcel Dekker Inc., New York, 2002).
[2] B. J.-C. Deboux, E. Lewis, P. J. Scully, and R. Edwards, J. Lightwave Technol. **13**, 1407 (1995).
[3] A. P. Ferreira, M. M. Werneck, and R. M. Ribeiro, Biosens. Bioelectron. **16**, 399 (2001).
[4] I. Del Villar, C. R. Zamarreño, M. Hernaez, F. J. Arregui, and I. R. Matias, Opt. Express **18**, 20183 (2010).
[5] M. Hernáez, I. Del Villar, C. R. Zamarreño, F. J. Arregui, and I. R. Matias, Appl. Opt. **49**, 3980 (2010).
[6] I. Del Villar, C. R. Zamarreno, P. Sanchez, M. Hernaez, C. F. Valdivielso, F. J. Arregui, and I. R. Matias, J. Opt. **12**, 095503 1 (2010).
[7] M. Smietana, J. Szmidt, M. Dudek, and P. Niedzielski, Diam. Relat. Mater. **13**, 954 (2004).
[8] J. Robertson, Mater. Sci. Eng., R **37**, 129 (2002).
[9] A. Shirakura, M. Nakaya, Y. Koga, H. Kodama, T. Hasebe, and T. Suzuki, Thin Solid Films **494**, 84 (2006).
[10] H. Voigt, F. Schitthelm, T. Lange, T. Kullick, and R. Ferretti, Sens. Actuators B **44**, 441 (1997).
[11] M. H. Oliveira, Jr., D. S. Silva, A. D. S. Cortes, M. A. B. Namani, and F. C. Marques, Diam. Relat. Mater. **18**, 1028 (2009).
[12] T. Tamulevičius, R. Šeperys, M. Andrulevičius, V. Kopustinskas, Š. Meškinis, and S. Tamulevičius, Thin Solid Films **519**, 4082 (2011).
[13] M. Śmietana, F. Akoa Oyono, J. Grabarczyk, and J. Szmidt, Proc. Eng. **47**, 1037 (2012).
[14] I. Del Villar, M. Hernaez, C. R. Zamarreño, P. Sánchez, C. Fernández-Valdivielso, F. J. Arregui, and I. R. Matias, Appl. Opt. **51**, 4298 (2012).
[15] Y. S. Dwivedi, A. K. Sharma, and B. D. Gupta, Appl. Opt. **46**, 4563 (2007).
[16] D. Ciprian and P. Hlubina, Proc. SPIE **8306**, 830612 (2011).
[17] F. Yang, and J. R. Sambles, J. Mod. Opt. **44**, 1153 (1997).
[18] M. Smietana, W. J. Bock, J. Szmidt, and J. Grabarczyk, Diam. Relat. Mater. **19**, 1461 (2010).
[19] M. Smietana, W. J. Bock, and J. Szmidt, Thin Solid Films **519**, 6339 (2011).

